Journal of Theoretical and Applied Mechanics, Sofia, Vol.51 (2021) pp. 335-351
SOLID MECHANICS

EFFECTS OF POROSITY AND PORE SIZE DISTRIBUTION ON THE COMPRESSIVE BEHAVIOUR OF PD BASED GLASS FOAMS

LUDMILA PARASHKEVOVA[1]*, LUDMIL DRENCHEV[2]

[1]*Institute of Mechanics, Bulgarian Academy of Sciences, Acad. G. Bonchev St., Block 4, 1113 Sofia, Bulgaria*

[2]*Institute of Metal Science, Equipment, and Technologies with Center for Hydro- and Aerodynamics "Acad. A. Balevski", Bulgarian Academy of Sciences, 67 Shipchenski prohod St., 1574 Sofia, Bulgaria*

[10 August 2020. Accepted: 05 April 2021]

ABSTRACT: The present work is devoted to the mechanical properties investigation of new materials with high porosity and an amorphous matrix. The technological parameters of obtaining 3D samples based on a palladium alloy and the results of uniaxial compression tests are presented. The synthesis of porous alloy Pd48Cu22Ni8Sb22 is realized by a two-step procedure with the boron acid as a foaming agent. An analytical homogenization for porous media is proposed taking into account the pore size distribution. The matrix is considered as a micropolar medium with an internal length which is assumed to be proportional to the molar volume of the alloy frozen in a glassy state. Numerical simulations are performed to clarify the role of pore size in predicting elastic moduli and onset of plastic flow.

KEY WORDS: closed-cell foam, homogenization, bulk metallic glass.

1 INTRODUCTION

Amorphous metals, discovered nearly 60 years ago and reported by Klement, Willens and Duwez in 1960, [1], currently are among the most actively studied metallic materials. They differ fundamentally from conventional metals in their atomic structure, mechanical properties, and solidification behaviour. Metallic glass-forming alloys vitrify under cooling (become "frozen" in a state similar to the liquid one) and form glasses. The glass transition involves no latent heat release and no discontinuous volume change. At the beginning , metallic glasses have been produced in the form of thin ribbons with a thickness of about 10 microns. In the last 20 years more and more alloy compositions have been elaborated and solid elements of several centimetres size (bulk metallic glasses) have been obtained. The diversity of bulk Metallic Glasses (MG) gives rise to an intensive research activity and the opportunity for

*Corresponding author e-mail: lusy@imbm.bas.bg

deeper understanding of liquids and of glasses in general. Moreover, they enlarge the possibilities for application of the amorphous metals in different industrial sectors. It could be expected that amorphous metals, especially bulk metallic glasses, will become a new-generation engineering materials [2, 3]. Due to their specific atomic arrangement MG are structurally different form crystalline counterpart and possess exceptional mechanical properties such as a wide range of fracture toughness (2055 MPam1/2) [4,5], large elastic strain limits (2%), and high yield strengths (2 GPa) [6]. Recently, metallic foams attract increasingly more interest as structural materials. To a large extent this is caused by the relatively high stiffness combined with very low specific weight and high energy-absorption capability. The unique combination of properties makes foams an attractive structural material, which can emulate the mechanical properties of natural foams, such as wood or bones, [7]. Foams can be classified in two main groups regarding their microstructure. Open-celled foams are characterized by interconnected voids and are mainly used as functional materials such as thermal and acoustic insulation. Closed-celled foams are characterized by spatially separated bubbles and find application as structural materials such as energy absorbers or lightweight stiff materials.

A combination of the specific properties of the bulk metallic glasses and foams uncover additional options for design of new materials with extraordinary characteristics. For example, since the amount of energy that can be absorbed scales with the strength of the material, bulk metallic glasses exhibiting a yield strength on the order of 2 GPa can be regarded as superior energy absorbers as compared to aluminium, which exhibits a strength of 250 MPa. Amorphous metallic foams are promising materials for application in medicine (surgical instruments, implants for bone replacement), mechatronics, aerospace industry and others. It could be expected that the next few years will bring serious advances, as we are on the threshold of exploiting new opportunities for microstructural design, opening up much broader application of the attractive materials formed from amorphous metals and their derivatives as amorphous metallic foams [8, 9]. In the present work an amorphous foam based on palladium , which combines the specific features of MG and a close cell foam is investigated theoretically and experimentally.

There are two aspects in the understanding dimensional effects associated with high porosity materials. The first aspect is related to the size of studied samples and the influence of this parameter on the mechanical and other characteristics (for example, heat transfer, permeability) of porous composites, see [10]. The effect of specimen size (relative to the cell size) on selected mechanical properties of aluminium foams is investigated in [11]. Models, described in [11], provide a physical basis for understanding size effects in metallic foams. The constrained deformation of an aluminium alloy foam sandwiched between steel substrates has been studded in [12]. It

has been proven that the yield strength increases with diminishing thickness of foam layer.

The second type of size effects is associated with a change in the properties of the porous macro-medium at different size distribution functions of closed pores. In one of the early works on this subject, [13] it as been obtained the decrease in Young's modulus and the compressive elastic buckling and plastic collapse stresses of a honeycomb with central voids at size increasing using finite element analysis. Recently Xue et al. [14], Xia et al. [15] investigated the effects of cell size on quasi-static compressive properties of magnesium alloy foams from the points of plateau stress, stress drop ratio. Their results showed that smaller cell size was beneficial to getting stable compressive process. In [16] the effect of the pore size distribution on the compressive behaviour for moderately expanded elastic polymer foams was studied. It was found that the compressive behaviour depends on the pore size distribution, especially in the collapse region. The wider cell distribution resulted in the higher stresses in the collapse region. In [17] Manoylov and co-authors suggested extended Vavakin & Salganik models in order to take into account various statistical distributions of pore sizes. Three modifications have been presented for materials with isolated spherical pores, merging pores modelled as ellipsoids and open pores.

In [18] Deverge, et al. have provided an experimental investigation of pore size effect on the linear viscolelastic properties of acoustic foams. It was noted by these authors that the shear modulus is inversely proportional to the square of the pore size.

So far in the literature there isn't a commonly accepted opinion on the issue of the effect of pore size on the elastic characteristics of closed-cell materials. In this paper, we propose a size-sensitive version of the two – steps homogenization procedure, accounting for the pore size distribution function. According to it the presence of pores which are commensurate with a certain micro structural parameter of the matrix can lead to an increase in classical Young's and shear moduli on the macro level. The progress of the idea for application of a Cosserat formulation in description of mechanical behaviour of foams could be seen in comparison with an earlier work [19].

2 Materials and Experiments

In order to have an appropriate material to test the models presented and its applicability we synthesized palladium (Pd) composition Pd48Cu22Ni8Sb22 which is an easy glass-forming alloy. The latter is foamed applying boric acid H_3BO_3 as foaming agent. The foam obtained is tested by AMSLER unit to find stress-strain curve not only for the high porosity material but for nominally non-porous one as well. On the basis of these curves yield stress for both kinds of samples are determined and the derived elastic parameters are used in model verification.

2.1 SYNTHESIS OF THE ALLOY AND FOAMING

The process of the alloy Pd48Cu22Ni8Sb22 synthesis is realized in two steps. In the first step Pd, Cu and Ni of purity in the range 99.95-99.99% are alloyed in electro-arc furnace under Ar (6N) purified by Ti as a getter. The obtained PdCuNi alloy is remelted in quartz ampoule displaced in induction coil together with appropriate quantity of Sn and dry B_2O_3. This process is realized in pure Ar (6N) atmosphere under pressure of 0.15 MPa. Afterwards, the obtained Pd48Cu22Ni8Sb22 alloy is foamed again in pure Ar (6N) atmosphere under pressure of 0.15 MPa. The foaming agent boric acid H_3BO_3 is put in the bottom of quartz ampoule and the alloy is placed over it. Then the ampoule is heated up to 1200 K. At that temperature the boric acid decomposes totally and evolves water. The water reacts with Sn and releases hydrogen and antimony oxide. The hydrogen plays the role of foaming gas. The rapid cooling and solidification of the foamed liquid is realized in flowing water at cooling velocity 100-120 K/min. Photos of a sample and the tomography image of the final porous material can be seen in Fig. 1 and Fig. 2.

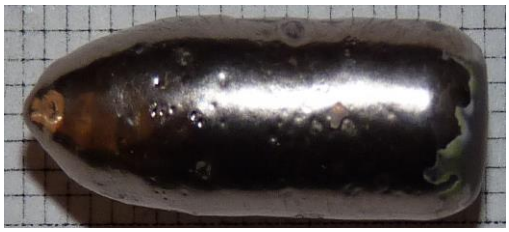

Fig. 1: An outside view of a foamed sample; grid scale 1 mm.

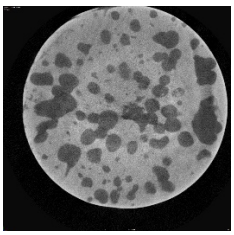

Fig. 2: Tomography image of a foamed sample microstructure.

2.2 STRESS-STRAIN CURVES AND YIELD STRESS OBTAINING

Compressive stress-strain curves are obtained for cylindrical samples with diameter $D_0 = 6.9$ mm and height $H_0 = 8.7$ mm, made from Pd48Cu22Ni8Sb22 alloy. The sample sizes are limited by the outer quartz ampoule. The specimen marked as S1, is nominally non-porous and the specimen of the second type, marked as S2, is porous with porosity $P = 0.31$, see Fig. 2. Using the curves shown in Fig. 3, the yield stress Rp0.2 for samples S1 and S2 are calculated and they are equal to 120.19 kg/mm^2 and 73.79 kg/mm^2, respectively. It could be seen that the yield stress of the porous material is approximately 60% lower than the yield stress of the non-porous one.

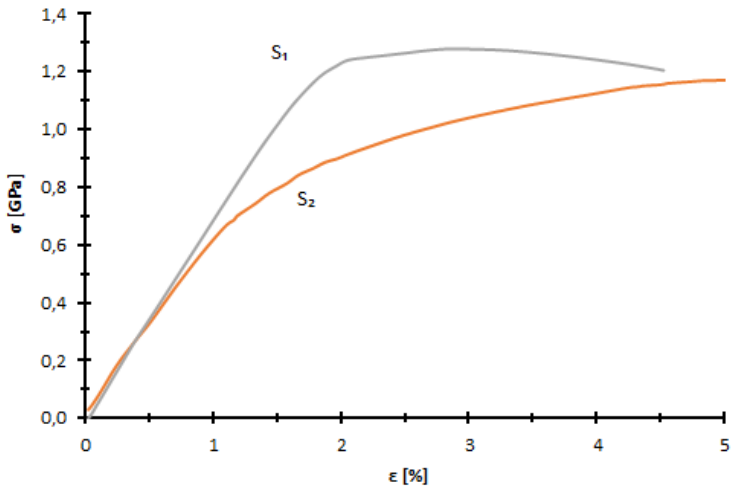

Fig. 3: Measured compressive stress-strain curves for nominally non-porous sample S1 and porous sample S2.

3 MODELLING

In this section the mechanical behaviour of metal-based foams under consideration is modelled following two-steps homogenization procedure for multiphase composite materials [20]. It is assumed that the foam could be regarded as a multiphase composite consisting of matrix and spherical inclusions which differ by size. The inclusions (pores) of a particular size form a separate phase. The overall response of the foam is elastic up to the certain value of the loading applied.

3.1 ELASTIC STATE

The matrix material is an isotropic micropolar centrosymmetric medium which is sensitive to internal rotations and the following elastic constitutive equations are valid for [21]:

$$
\begin{aligned}
&\sigma'_{(ij)} = 2G_m\varepsilon'_{(ij)} \quad \sigma_{\langle ij\rangle} = 2\varkappa\varepsilon_{\langle ij\rangle} \quad \sigma_{(kk)} = 3K_m\varepsilon_{(kk)} \\
&m'_{(ij)} = 2\beta k'_{(ij)} \quad\quad m_{\langle ij\rangle} = 2\gamma k_{\langle ij\rangle} \quad m_{(kk)} = 3Nk_{(kk)}.
\end{aligned} \tag{1}
$$

The stress and strain measures are $\sigma_{ij} = \sigma_{(ij)} + \sigma_{\langle ij\rangle}$; $\varepsilon_{ij} = \varepsilon_{(ij)} + \varepsilon_{\langle ij\rangle}$, couple stress and curvature tensor $m_{ij} = m_{(ij)} + m_{\langle ij\rangle}$; $k_{ij} = k_{(ij)} + k_{\langle ij\rangle}$, respectively. Everywhere in the paper $\{...\}'_{ij}$ is the notation for a tensor deviator. Symbols $(...)$ and $\langle...\rangle$ in the subscripts denote symmetric and anti-symmetric parts of a tensor. Among

Cauchy (shear modulus G_m and bulk modulus K_m) and Cosserat model parameters the following relations are adopted:

$$l_m{}^2 = \beta/G_m = \gamma/\varkappa\,, \quad \varkappa/G_m = \gamma/\beta = p. \tag{2}$$

If $p = 1$ one gets a simpler variant of the theory, which is applied further on, where:

$$\varkappa = G_m\,, \quad \gamma = \beta = l_m{}^2 G_m\,, \quad N = l_m{}^2 K_m\,, \tag{3}$$

l_m is an internal length of the matrix and the index m is set for the matrix properties.

After homogenization the composite, however, is a classic Cauchy-type material. This is assumption of consequence, it simplifies the estimation of overall properties allowing some size effects to be kept in an average manner.

The two-steps homogenization procedure is based on Pierard et al. approach [22].

According to it the composite Representative Volume Element (RVE) is rearranged virtually into a set of pseudograins. Each pseudograin is a two-phase composite containing matrix and pores of a particular size; the volume fraction of pores in it is equal to the total porosity C.

Throughout the article, the term "total porosity" or "total pore concentration" means the total volume fraction of all pores in the RVE regardless of their size.

Here as a first step a Size-Sensitive variant of Generalized Mixture Rule (SSGMR) is used as a method of homogenization for every pseudograin.

The elastic moduli predictions are calculated by analytical approach based on the Generalized Mixture Rule (GMR). The explicit formulae for the bulk and shear moduli are obtained on the base of the phenomenological mixture rule [23] coupled to Size-Sensitive variant of Mori-Takaka (SSMT) approach [20]. Supposing that the linear approximations of GMR and SSMT about the total porosity coincide, it is possible to get the exponents α_K and $\alpha_G(D_i)$ as particular expressions, which depend only on the matrix Poisson's ratio and the size-sensitive parameter b_{0i}.

So, the homogenized properties of a pseudograin with pores of size D_i are estimated by means of the formulae [24]:

$$K_{ci} = K_c = K_m(1-C)^{\alpha_K}, \tag{4}$$

$$G_{ci}(D_i) = G_m(1-C)^{\alpha_G(D_i)}; \tag{5}$$

$$\alpha_K = \frac{3(1-\nu_m)}{2(1-2\nu_m)}\,, \quad \alpha_G = \frac{15(1-\nu_m)}{(7-5\nu_m)+15(1-\nu_m)b_{0i}}\,,$$

where ν_m is matrix Poisson's ratio. The size-sensitive parameter b_{0i} depends on the micropolar properties of the matrix material and on the pore diameter D_i:

$$b_{0i} = \frac{6p}{5\,(p+1)} R_i\,(\eta_i)\,, \tag{6}$$

$$R_i(\eta_i) = e^{-\eta_i}\left(\eta_i^{-2} + \eta_i^{-3}\right)(\eta_i ch\eta_i - sh\eta_i)\ , \quad \eta_i = \frac{\sqrt{p}}{(p+1)}\frac{D_i}{l_m}.$$

In general, $0 \le b_{0i} \le 2/5$, but if $p = 1$, $0 \le b_{0i} \le 1/5$.

On the second step, the set of pseudograins in the RVE is subjected to Budynski–Hill self-consistent procedure, developed for polycrystals and modified in [20]. The overall bulk and shear moduli of the porous composite are obtained as solutions $\overline{K}$, $\overline{G}$ of the following non-linear system of equations:

$$(7)\quad \sum_i \frac{\tilde{C}_i}{1-\dfrac{3\overline{K}}{3\overline{K}+4\overline{G}}\left(1-\dfrac{K_c i}{\overline{K}}\right)} - 1 = 0, \quad \sum_i \frac{\tilde{C}_i}{1-\dfrac{6(\overline{K}+2\overline{G})}{5(3\overline{K}+4\overline{G})}\left(1-\dfrac{G_{ci}}{\overline{G}}\right)} - 1 = 0,$$

$$(8)\qquad \tilde{C}_i = C_i(D_i)/C \qquad \sum_i C_i = C\,.$$

In some cases too many different pore sizes are observed and they could be adequately represented by the corresponding density distribution function $\psi(D)$, such that the condition $\int_0^\infty \psi(D)dD = 1$ is satisfied. Then, the system (7) takes the form

$$(9)\quad \begin{aligned} &\int_0^\infty \frac{\psi(D)dD}{1-\dfrac{3\overline{K}}{3\overline{K}+4\overline{G}}\left(1-\dfrac{K_c(D)}{\overline{K}}\right)} - 1 = 0\,; \\ &\int_0^\infty \frac{\psi(D)dD}{1-\dfrac{6(\overline{K}+2\overline{G})}{5(3\overline{K}+4\overline{G})}\left(1-\dfrac{G_c(D)}{\overline{G}}\right)} - 1 = 0\,. \end{aligned}$$

If one takes into account (4) and (8), the system (7) is transformed to only one equation about $\overline{G}$, which should be solved numerically

$$(10)\qquad \overline{K} = K_c\,, \quad \sum_i \frac{C_i(D_i)}{1-\dfrac{6(K_c+2\overline{G})}{5(3K_c+4\overline{G})}\left(1-\dfrac{G_{ci}}{\overline{G}}\right)} - C = 0.$$

Let's note that for the special values of the matrix Poisson's ratio:

$$\nu_m^* = \frac{1-5b_{0i}}{5(1-b_{0i})}\,, \quad \alpha_G = \alpha_K = \frac{3(1-\nu_m^*)}{2(1-2\nu_m^*)},$$
$$\overline{G} = G_c\,, \quad \overline{K} = K_c\,, \quad K_c/K_m = G_c/G_m\,, \quad \overline{\nu} = \nu_c = \nu_m^*.$$

3.2 INITIAL PLASTIC STATE

It is commonly adopted that the plastic state of the material occurs when an irreversible part of the deformation appears. Further development of this state is determined by the brittleness or ductility properties. For metals there exists a relationship between the elastic Poisson's ratio, and the fragility of the material. Another interpretation of such a relation is the dependence of plastic properties on the bulk/ shear moduli ratio [25]. According to it, the shear stress at yielding of bulk metallic glass is approximately 0.02 to 0.027 of shear elastic modulus. If this relation is rearranged applying the common connection between uniaxial compression stress and shear stress, one gets

$$\sigma_{pm} = \sqrt{3}\tau_{pm} \approx \sqrt{3}(0.02 - 0.027)G_m \approx (0.035 - 0.045)G_m \,. \tag{11}$$

In this paper, we present in details a condition which defines the transition from elastic to plastic state of the porous composite at the macro level, based on the averaged characteristics of the micropolar matrix. It is supposed that the plastic state at a particular point of the micropolar material (in the matrix) occurs at a combination of stresses such that the effective stress defined by the equation below reaches a certain value.

$$\sigma_e^2 = \frac{1}{2}\sigma'_{(ij)}\sigma'_{(ij)} + \frac{1}{2l_m^2}m'_{(ij)}m'_{(ij)} + \frac{1}{2l_m^2}m'_{<ij>}m'_{<ij>} = {\tau_{pm}}^2 \,. \tag{12}$$

In the case of a porous composite with a certain microstructure described by RVE, we assume that a non-elastic plastic state occurs if the effective stress averaged over the matrix volume part of the RVE reaches the same critical value

$$\langle\sigma_e^2\rangle_m = \left\langle \frac{1}{2}\sigma'_{(ij)}\sigma'_{(ij)} + \frac{1}{2l_m^2}m'_{(ij)}m'_{(ij)} + \frac{1}{2l_m^2}m'_{\langle ij\rangle}m'_{\langle ij\rangle} \right\rangle_m = {\tau_{pm}}^2. \tag{13}$$

Let's fictitiously replace pores with isotropic elastic inclusions with very low elastic moduli. In addition, we suggest that in the case of closed porosity under consideration (or factious inclusions embedded into the matrix), the deformations of the composite are controlled by the deformations of the matrix as it is a stronger phase. The stiffer is the matrix the smaller are the strains on the pore contours and the smaller are the changes of the pore shape.

The following relations between the averaged strain measures is accepted

$$\langle\frac{1}{2}\varepsilon_{ij}\varepsilon_{ij}\rangle_m = \left\langle\frac{1}{2}\varepsilon_{(ij)}\varepsilon_{(ij)} + \frac{1}{2}\varepsilon_{\langle ij\rangle}\varepsilon_{\langle ij\rangle}\right\rangle_m = \left\langle\frac{1}{2}\varepsilon_{ij}\varepsilon_{ij}\right\rangle_{in} = \frac{1}{2}E_{ij}E_{ij} \tag{14}$$

$$C_m\langle\varepsilon_{(kk)}\rangle_m + C_{in}\langle\varepsilon_{kk}\rangle_{in} = E_{kk} \,. \tag{15}$$

To relate the states of the composite at the micro and macro levels, we use Hill's equation for the balance of elastic energy W:

$$\begin{gathered}\langle W\rangle_{\text{RVE}} = C_m\langle W\rangle_m + C_{in}\langle W\rangle_{in} = \overline{W};\\ \langle W\rangle_m = \left\langle \frac{1}{2}\sigma_{ij}\varepsilon_{ij} + \frac{1}{2}m_{ij}k_{ij}\right\rangle_m; \quad \langle W\rangle_{in} = \left\langle \frac{1}{2}\sigma_{ij}\varepsilon_{ij}\right\rangle_{in};\\ \overline{W} = \frac{1}{2}\Sigma_{ij}E_{ij}\,.\end{gathered} \tag{16}$$

We use substantially the assumption that at the macro level the homogenized material is of Cauchy type. Volume averaging over RVE leads to the fact that the parts associated with micropolar quantities, averaged over the matrix, are equal to zero, since no micropolar properties are considered in the inclusions volume and at the macro level. More specifically, one gets

$$\begin{gathered}\left\langle \frac{1}{2}\sigma_{\langle ij\rangle}\sigma_{\langle ij\rangle}\right\rangle_m = 0\,, \quad \left\langle \frac{1}{2}\varepsilon_{\langle ij\rangle}\varepsilon_{\langle ij\rangle}\right\rangle_m = 0\,,\\ \left\langle \frac{1}{2}m'_{\langle ij\rangle}m'_{\langle ij\rangle}\right\rangle_m = \left\langle \frac{1}{2}m_{\langle ij\rangle}m_{\langle ij\rangle}\right\rangle_m = 0\,, \quad \langle {m_{kk}}^2\rangle_m = 0\,.\end{gathered}$$

In this way, equation (16) and (13) take the simpler forms

$$\begin{aligned}&C_m\left\langle \frac{1}{2G_m}{\sigma'}_{(ij)}{\sigma'}_{(ij)} + \frac{1}{9K_m}\sigma^2_{(kk)}\right\rangle_m\\ &\quad + C_{in}\left\langle \frac{1}{2G_{in}}{\sigma'}_{ij}{\sigma'}_{ij} + \frac{1}{9K_{in}}\sigma^2_{kk}\right\rangle_{in} = \left\langle \frac{1}{2\overline{G}}{\Sigma'}_{ij}{\Sigma'}_{ij} + \frac{1}{9\overline{K}}\Sigma^2_{(kk)}\right\rangle.\end{aligned} \tag{17}$$

$$\langle\sigma_e^2\rangle_m = \left\langle \frac{1}{2}{\sigma'}_{(ij)}{\sigma'}_{(ij)}\right\rangle_m = {\tau_{pm}}^2\,. \tag{18}$$

Upon the onset of the plastic state, the condition (18) is fulfilled, but the inclusions are deformed, remaining elastic. Additionally (14, 15) should be applied into (17). Thus, using the energy balance equation, it is possible to obtain the initial condition for the plastic state expressed in stresses at the macro level. If one let $G_{in} \longrightarrow 0$; $K_{in} \longrightarrow 0$, the final form of the yield condition for homogenized porous material is presented by equation (19)

$$\frac{3}{2}\Sigma'_{ij}\Sigma'_{ij} + \boldsymbol{A}^2\frac{\Sigma^2_{kk}}{9} = \boldsymbol{H}^2{\sigma_{pm}}^2, \tag{19}$$

where

$$\boldsymbol{A}^2 = 2\frac{\left[(1-C) - \frac{\overline{K}}{K_m}\right]}{\left[(1-C) - \frac{2}{3}\frac{\overline{G}}{K_m}\right]}\frac{\overline{G}^2}{\overline{K}^2}\,, \quad \boldsymbol{H}^2 = \frac{(1-C)\left[1 - \frac{2}{3}\frac{G_m}{K_m}\right]}{\left[(1-C) - \frac{2}{3}\frac{\overline{G}}{K_m}\right]}\frac{\overline{G}^2}{{G_m}^2}\,.$$

In (19) C is the total porosity, $\overline{K}$ and $\overline{G}$ are the solutions of the system (7) or (9). In calculation of the overall elastic moduli size effects are taken into account through the homogenization scheme adopted. These effects are caused by the reaction of the micropolar matrix to the presence of pores embedded in it. The condition (19) is applicable, if $\nu_m > 0$, the matrix Poisson's ratio has a positive value.

4 Numerical Results and Model Parameters Study

To identify the effect of pore size on the elastic and initial plastic state of the high porosity composite, numerical simulations of two types of metallic foams with different pore distribution were performed. The spherical pores in a foam are divided into two groups, which are very different in size. Such a pore size distribution in the modeled RVE is illustrated in Fig. 4. The first group can be called the group of large pores with an average size D and volume fraction $C_1(D)$, and the second group of small pores with volume fraction $C_2(d)$; $C_1(D) + C_2(d) = C$. The average size of small pores is commensurate with the thickness of the matrix walls. Mathematically, this is expressed by the condition $d \approx 2l_m$. As in many applications of the micropolar theory it is supposed that $p = 1$, see (2) and (3). If $d \approx 2l_m$ and $p = 1$, than according to (6) $b_{0i} = 0.1624$.

We compare two ways of porosity increasing for metal foams. In all cases the maximum volume fraction of each group does not exceeded the packing limit concentrations known for the mono-size composite. These critical values depend on pores spatial distribution. Cubic close-packing (FCC) and hexagonal close-packing (HCP) arrangements are densest sphere-packing in three-dimensions [26].

For equal spheres the densest packing uses approximately 74% of RVE volume. A random packing generally has a density about 64%, so it is suggested that $C_i < C^* < 0.64$, $i = 1, 2$.

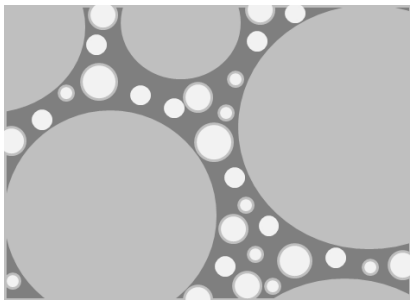

Fig. 4: Schematic image of porous microstructure and two kinds of pores with average diameter D and d, $D \ll d$.

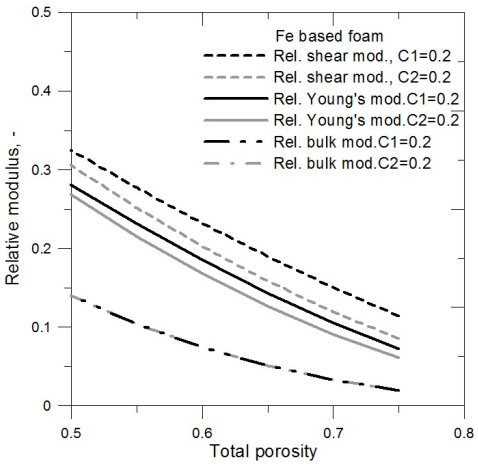

Fig. 5: Comparison of model predictions for the relative elastic moduli of Fe based foam at variation of the composite porosity and $C_1 = 0.2$, $C_2 = C - C_1$ and $C_2 = 0.2$, $C_1 = C - C_2$, $\nu_m = 0.32$, $K_m = 200$ GPa.

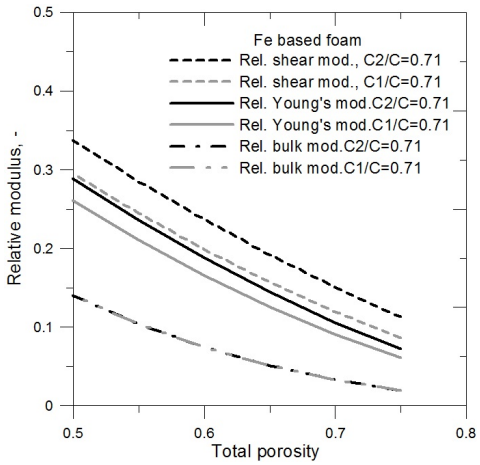

Fig. 6: Comparison of model predictions for the relative elastic moduli of Fe based foam at variation of the composite porosity and $C_1/C = 0.71$, $C_2 = C - C_1$ and $C_2/C = 0.71$, $C_1 = C - C_2$, $\nu_m = 0.32$, $K_m = 200$ GPa.

In the first case the volume fraction of one pore phase is kept constant but the volume fraction of the other pore phase is increasing along with the total porosity as $C = C_1 + C_2$. Higher values for Young's and shear moduli are calculated when the amount of small pores is increasing and this tendency is illustrated in Fig. 5 for iron (Fe) based foam with $\nu_m = 0.32$, $K_m = 200$ GPa [27] at $C_1 = 0.2$, $C_2 = C - C_1$ and $C_2 = 0.2$, $C_1 = C - C_2$.

In the second case the relative volume fraction of one pore phase is kept constant when the total porosity is increasing, $C_1/C = \text{const}$, or $C_2/C = \text{const}$. The changes of relative moduli with porosity at $C_1/C = 0.71$, $C_2 = C - C_1$ and $C_2/C = 0.71$, $C_1 = C - C_2$ are presented in Fig. 6 for Fe based foam and in Fig. 7 for Pd based foam with $\nu_m = 0.4$, $K_m = 170$ GPa [9, 28]. According to the model, see (10), the composite bulk modulus depends only on porosity. The hardening size effect of small pores is the most pronounced for shear modulus. Young's modulus is higher for composites with predominant small size pores and at the same time it is more sensitive to matrix Poisson's ratio.

In Fig. 8 the model predictions of the relative uniaxal compressive yield limit for Pd based alloys at different porosities are shown. The matrix Young's modulus is 102 GPa, Poisson's ratio is 0.4. The solid curve corresponds to the case of a

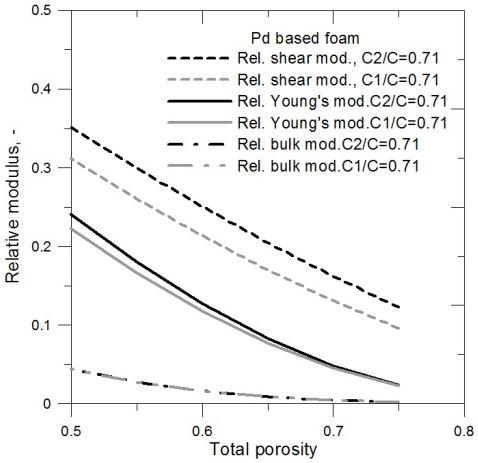

Fig. 7: Comparison of model predictions for the relative elastic moduli of Pd based foam at variation of the composite porosity and $C_1/C = 0.71$, $C_2 = C - C_1$ and $C_2/C = 0.71$, $C_1 = C - C_2$, $\nu_m = 0.4$, $K_m = 170$ GPa.

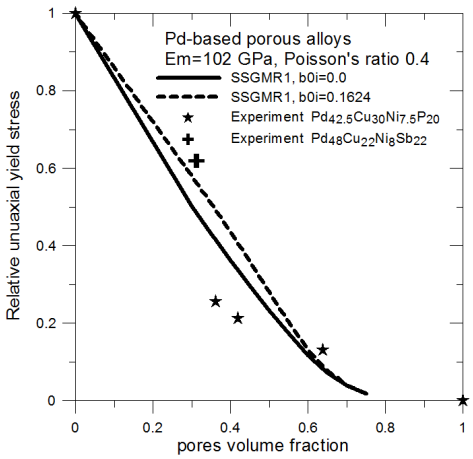

Fig. 8: Model dependence of the relative uniaxial yield stress on porosity. Comparisons with experiments on porous Pd alloys: Pd42.5Cu30Ni7.5P20 from [3]; Pd48Cu22Ni8Sb22 – present work.

composite with very big pores ($b_{0i} = 0.0$) and the dashed line – to the case of small pores ($b_{0i} = 0.1624$) only.

Also, we can compare the yield limit obtained for our Pd48Cu22Ni8Sb22 alloy, see Section 2.2 and phenomenological relationship (11) suggested by Zhang [25]. For Pd bulk glassy alloys (Young's modulus 90–100 GPa, Poisson's ratio 0.39–0.41) the compressive yield limit should be about (1.05–1.64) GPa and our test data fall into this interval.

The effect of the amount of small pores during the transition from elastic to non-elastic state of a two-dimensional porous composite significantly varies for different types of macrostressed state. As can be seen from Fig. 9, the model predicts that the closer the stress state to the pure shape change, the stronger the size effect and the closer the stress state to equiaxial deformation, the effect disappears. At least one can expect that foams with a larger volume of small pores will be more resistant to torsion than foams with coarse pores. For the uniaxial compression process, the calculations show that, in accordance with the accepted model, the hardening effect associated with the presence of a larger number of small pores will decrease with an increase in the total porosity, see the black straight line in Fig. 9.

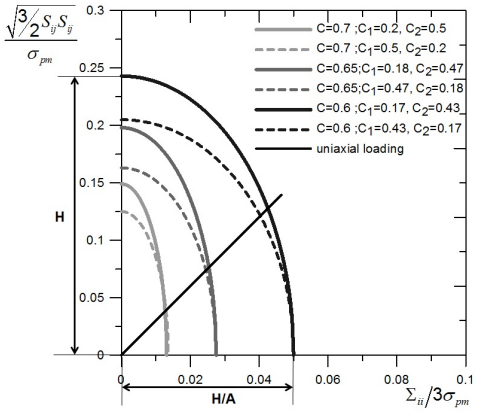

Fig. 9: Projections of the initial yield surfaces for porous Pd composite in relative mean stress–deviatoric stress plane at variation of the composite porosity and $C_1/C = 0.71$, $C_2 = C - C_1$ and $C_2/C = 0.71$, $C_1 = C - C_2$, $\nu_m = 0.4$, $K_m = 170$ GPa.

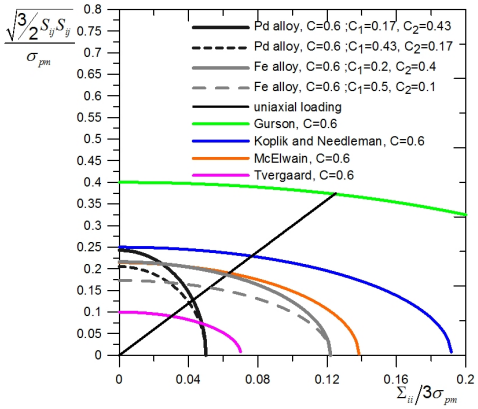

Fig. 10: Models comparison: projections of the initial yield surfaces in relative mean stress–deviatoric stress plane at total porosity $C = 0.6$. Present model: black curves – for Pd based alloy; grey curves – for Fe based alloy.

We selected the widely popular series of models based on Gurson's relation [29] to show how the present model for the beginning of plastic flow correlates with other known models. This set of models can be described by the following expression with different coefficients q_1, q_2, suggested by different authors [30]:

$$\left(\frac{\Sigma_{eq}}{\sigma_{pm}}\right)^2 + 2q_1 C \cosh\left(\frac{1}{2} q_2 \frac{\Sigma_{kk}}{\sigma_{pm}}\right) - {q_1}^2 C^2 - 1 = 0; \tag{20}$$

$$\Sigma_{eq} = \sqrt{\frac{3}{2}\Sigma'_{ij}\Sigma'_{ij}}\,.$$

In dimensionless coordinates Fig. 10 shows the results calculated by means of (19) for two porous alloys: a) based on palladium (continuous and discontinuous curves in black) and b) based on iron (continuous and discontinuous curves in grey colour).

For comparison, models of other four authors are shown (each with only one curve for both cases, since all these models determine the initial plastic state depending only on the yield strength of the matrix material and on the total porosity). Gurson's model [29] $q_1 = 1$, $q_2 = 1$, is represented by the green line, Tvergaard's model [31] $q_1 = 1.5$, $q_2 = 1$ – by a purple curve; Koplik-Needleman's model [32] $q_1 = 1.25$,

$q_2 = 1$ – by a blue curve; McElwain's model [33] $q_1 = 1.31$, $q_2 = 1.16$ – by an orange curve. All curves correspond to total porosity $C = 0.6$.

It is important to note that the analytical yield criterion (19) presented herein demonstrates obvious flexibility with respect to various materials and, most importantly, all model parameters are clearly defined as physical characteristics: they are elastic matrix moduli and effective elastic composite moduli, along with the already mentioned matrix yield strength and total pore concentration.

5 Concluding Remarks

Amorphous materials like Pd based glass foams are modelled as composites of high porosity where the matrix phase is considered as Cosserat continuum. The presented variants of the generalized mixture rule, see (4, 9) are incorporated into a pore size sensitive homogenization procedure and takes into account the density distribution function of pores diameters.

The numerical simulations provided show that the adopted models are appropriate to capture the main elastic plastic features of the materials under consideration. But like other micropolar theories applications, a reasonable question arises herein: which microstructure parameter of the matrix could be regarded as the internal length parameter l_m? The answer is of particular importance as the ratio D_i/l_m determines the pore size influence on the overall properties predictions.

As far as we deal with an amorphous glass-like matrix, we suggest that the internal length parameter l_m is correlated to the molar volume V_{mol} of the matrix alloy, so

$$l_m \sim (V_{\text{mol}})^{1/3}\,, \tag{21}$$

where the molar volume is defined by the ratio of the molar mass versus density and the atoms arrangement in the amorphous alloy reflects on the molar volume. There exist many evidences confirming the influence of the molar volume (as a space microstructure characteristic) on the elastic constants, see [34]. Additional research is need to clarify the exact form of the relation (21).

With respect to the foam production method used for Pd48Cu22Ni8Sb22 alloy, the processing conditions will be improved to obtain a more uniform pore distribution throughout the entire volume of 3D samples.

Acknowledgements

This research is carrying out in the frame of KMM-VIN – European Virtual Institute. All equipment for materials characterization used in this work was funded by the European Regional Development Fund within the OP 'Science and Education for Smart Growth 2014–2020', project No BG05M2OP001-1.001-0008-C08. The financial support of BG FSI through the grant DH 07/17/2016 'New approach for structure

and properties design of amorphous and nanostructured metallic foams' is gratefully acknowledged.

REFERENCES

[1] W. KLEMENT, R.H. WILLENS, P. DUWEZ (1960) Non-crystalline structure in solidified goldsilicon alloys. *Nature* **187** 869-870.

[2] W.L. JOHNSON (2002) Bulk amorphous metal – An emerging engineering material. *Journal of the Minerals, Metals and Materials Society* **54** 40-43.

[3] T. WADA, A. INOUE (2004) Formation of porous Pd-based bulk glassy alloys by a high hydrogen pressure melting-water quenching method and their mechanical properties. *Materials Transactions* **45**(8) 2761-2765.

[4] P. LOWHAPHANDU, J.J. LEWANDOWSKI (1998) Fracture toughness and notched toughness of bulk amorphous allo Zr-Ti-Ni-Cu-Be. *Scripta Materialia* **38** 1811-1817.

[5] C.J. GILBERT, R.O. RITCHIE, W.L. JOHNSON (1997) Fracture toughness and fatigue-crack propagation in a Zr-Ti-Ni-Cu-Be bulk metallic glass. *Applied Physics Letters* **71** 476-478.

[6] H.A. BRUCK, T. CHRISTMAN, A.J. ROSAKIS, W.L. JOHNSON (1994) Bruck, H., A., Christman, T., Rosakis, A.,J., Johnson, W.,L.: Quasi-static constitutive behavior of Zr41.25Ti13.75Ni10Cu12.5Be22.5 bulk amorphous-alloys. *Scripta Metallurgica et Materialia* **30** 429-434.

[7] L. DRENCHEV, J. SOBCZAK (2014) "Self-healing materials as biomimetic smart structures". Foundry Research Institute, Krakov, ISBN 978-83-88770-98-2.

[8] A. LINDSAY GREER (2009) Metallic glasses... on the threshold. *Materials Today* **12** 14-22.

[9] WEI HUA WANG (2012) The elastic properties, elastic models and elastic perspectives of metallic glasses. *Progress in Materials Science* **57** 487-656.

[10] C. TEKOGLU, L.J. GIBSON, T. PARDOEN, P.R. ONCK (2011) Size effects in foams: Experiments and modeling. *Progress in Materials Science* **56** 109-138.

[11] E. ANDREWS, G. GIOUX, P.R. ONCK, L.J. GIBSON (2001) Size effects in ductile cellular solids. Part II: Experimental results. *International Journal of Mechanical Sciences* **43** 701-713.

[12] C. CHEN, N. FLECK (2002) Size effects in the constrained deformation of metallic foams. *Journal of the Mechanics and Physics of Solids* **50** 955-977.

[13] X.E. GUO, L.J. GIBSON (1999) Behavior of intact and damaged honeycombs: a finite element study. *International Journal of Mechanical Sciences* **41** 85-105.

[14] Z.G. XU, J.W. FU, T.J. LUO, Y.S. YANG (2012) Effects of cell size on quasi-static compressive properties of Mg alloy foams. *Mater Design* **34** 40-44.

[15] X.C. XIA, X.W. CHEN, Z. ZHANG, X. CHEN, W.M. ZHAO, B. LIAO, B. HUR (2013) Effects of porosity and pore size on the compressive properties of closed-cell Mg alloy foam. *Journal of Magnesium and Alloys* **1**(4) 330-335.

[16] TAKASHI UNEYAMA, TATSUYA YAMAZAKI, TOSHIO IGARASHI, KOHHEI NITTA (2019) Effect of pore size distribution on compressive behavior of moderately expanded lowdensity polyethylene foams. *Polymer Engineering and Science* **59**(3) 510-518.

[17] A.V. MANOYLOV, F.M. BORODICH, H.P. EVANS (2013) Modelling of elastic properties of sintered porous materials. *Proceedings of the Royal Society of London. Series A, Mathematical and Physical Sciences* **469** 20120689.

[18] M. DEVERGE, L. BENYAHIA, S. SAHRAOUI (2009) Experimental investigation on pore size effect on the linear viscolelastic properties of acoustic foams. *Journal of the Acoustical Society of America* **126**(3) 93-96.

[19] S. DIEBELS, H. STEEB (2002) The size effect in foams and its theoretical and numerical investigation. *Proceedings of the Royal Society of London. Series A, Mathematical and Physical Sciences* **458** 2869-2883.

[20] L. PARASHKEVOVA, L. DRENCHEV, P. EGIZABAL (in print) Mechanical properties assessments for materials of high porosity and light alloys with predominant embedded phases. Computing in Industrial Mathematics, BGSIAM 2018, Studies in Computational Intelligence.

[21] W. NOWACKI (1986) "Theory of asymmetric elasticity". Pergamon Press.

[22] O. PIERARD, C. FRIEBEL, I. DOGHRI (2004) Mean-field homogenization of multi-phase thermo-elastic composites: a general framework and its validation. *Composites Science and Technology* **64** 1587-1603.

[23] S. JI, QI GU, B. XIA (2006) Porosity dependence of mechanical properties of solid materials. *Journal of Materials Science* **41** 1757-1768.

[24] L. PARASHKEVOVA (2020) Characterization of porous media by a size-sensitive homogenization approach. *Journal of Theoretical and Applied Mechanics – Sofia* **50** 338-353.

[25] ZHIYING ZHANG (2008) Elastic properties of bulk-metallic glasses studied by resonant ultrasound spectroscopy. PhD thesis, University of Tennessee.

[26] T.C. HALES (1992) The sphere packing problem. *Journal of Computational and Applied Mathematics* **44**(1) 41-76.

[27] C. SURYANARAYANA, A. INOUE (2013) Iron-based bulk metallic glasses. *International Materials Reviews* **58**(3) 131-166.

[28] A. INOUE, A. TAKEUCHI (2002) Recent progress in bulk glassy alloys. *Materials transactions, JIM* **43** 1892-1906.

[29] A. GURSON (1977) Continuum theory of ductile rupture by voidnucleation and growth, part I, yield criteria and flow rules for porous ductile media. *Journal of Engineering Materials and Technology* **99** 2-15.

[30] A. BOURIH, W. KADDOURI, T. KANITA, S. MADANI, A. IMAD (2017) Effective yield surface of porous media with random overlapping identical spherical voids. *Journal of Materials Research and Technology* **7**(2) 103-117.
DOI: 10.1016/j.jmrt.2017.01.002.

[31] V. TVERGAARD (1982) On localization in ductile materials containing spherical voids. *International Journal of Fracture* **18**(4) 237-252.

[32] J. KOPLIK, A. NEEDLEMAN (1988) Void growth and coalescence in porous plastic solids. *International Journal of Solids and Structures* **24** 835-853.

[33] D.L.S. MCELWAIN, A. ROBERTS, A. WILKINS (2006) Yield criterion of porous materials subjected to complex stress states. *Acta Materialia* **54** 1995-2002.

[34] J.Q. WANG, W.H. WANG, H.B. YU, H.Y. BAI (2009) Correlations between elastic moduli and molar volume in metallic glasses. *Applied Physics Letters* **94** 121904.